

Nonthermal Melting Unravalled by Realistic Excitation and Nonadiabatic Dynamics

Chao Lian,¹ S. B. Zhang,^{2,*} and Sheng Meng^{1,3,†}

¹*Beijing National Laboratory for Condensed Matter Physics and Institute of Physics, Chinese Academy of Sciences, Beijing, 100190, P. R. China*

²*Department of Physics, Applied Physics, and Astronomy, Rensselaer Polytechnic Institute, Troy, New York 12180, USA*

³*Collaborative Innovation Center of Quantum Matter, Beijing, 100190, P. R. China*

(Dated: May 24, 2022)

Ultrafast electron-nuclear dynamics in silicon upon laser excitation has been investigated using real-time time-dependent density functional theory. With excitation conditions that account for experimental optical spectra and nonadiabatic electron-phonon effects naturally included, we observe for the first time intrinsic nonthermal melting of Si within 200 fs at a temperature $T < 600$ K, far below the thermal melting temperature of 1680 K. Both excitation threshold and time evolution of diffraction intensity agree well with experiments. Nonthermal melting is attributed to an excitation-induced drastic change in bonding electron density and subsequently a decrease in the melting barrier, rather than lattice heating as previously assumed by the two-temperature model.

PACS numbers: 78.47.J-, 63.20.kd, 64.60.Cn, 71.15.Mb

Materials can exhibit exotic behaviors and dynamics different from ground state when excited by laser light. Laser excitation generates unique condensed phases of matter[1], such as nonthermal melting[2–12], warm dense matter[13, 14], and microexplosion[15, 16]. They are of great importance to various applications including micromachining, shock wave generation, and novel phases existing only in the core of large planets[1]. The challenge is to modify electronic interactions in photoexcited materials in a controlled way. Building a general theoretical framework for laser modified phases and ultrafast behaviors is thus of great importance.

A popular example is nonthermal melting. Melting within an ultrafast timescale upon photoexcitation has been ubiquitously observed in a wide range of semiconductors Si [2, 3], Ge [4], GaAs [5, 6], InSb [7, 8], Ge₂Sb₂Te₅[9, 10], and most recently in two dimensional materials such as TiSe₂ [11] and TaS₂ [12]. The duration of nonthermal melting process is short (100 fs to 1 ps), not sufficient for the crystal lattice to be heated [17]. Therefore the lattice remains cold compared to the high thermal melting temperature.

Despite extensive experimental and theoretical investigations in past three decades, the atomistic mechanism of nonthermal melting remains controversial. In experiment, plasma annealing (PA), namely the lowering in melting barrier by laser excitation was phenomenologically invoked to explain low temperature melting [3, 7]. It lacks, however, direct evidences due to missing information of potential energy surface in excited states. First-principles atomistic simulations in principle could provide such information, however, previous theoretical works fail to yield convincing analysis: In such studies a rapid increase in lattice temperature (10^2 K \rightarrow 10^3 K in 100 fs) is essential to induce melting [18–20], implying that laser-induced melting is in fact a thermal process.

The inconsistency originates from severe limitations in the current state-of-the-art theory and simulation of nonthermal melting. There are two major challenges. The first is the treatment of initial excitation. The two-temperature model (TTM) is prevalent in literature to describe electronic excitation [18–22]. The basic assumption is that under laser illumination the occupation of respective electronic states adopts an equilibrium Fermi-Dirac distribution at the elevated electronic temperature ($T_e \sim 10^4$ K), significantly higher than the concurrent ionic temperature of the crystal ($T \sim 10^2$ K). However, this assumption conflicts with the fact that hot electrons and holes take at least 10^2 to 10^3 fs to fully relax into a quasi-equilibrium state with a well-defined T_e [17]. Thus T_e is ill-defined and could be irrelevant during ultrafast melting (~ 100 fs). A new physical model is urgently needed to describe hot electrons and their ultrafast relaxation in a regime far from equilibrium. Another challenge is the inclusion of nonadiabatic effects such as electron-phonon (el-ph) coupling. Relying on Born-Oppenheimer approximation (BOA), such effects are ignored in TTM simulations[18, 19, 21], despite of a few attempts to introduce empirical parameters to account for nonadiabatic effects [20, 22]. Since nonadiabatic coupling determines the pathway and dynamics of ultrafast energy transfer, a nonadiabatic framework instead of BOA is desirable in simulating nonthermal melting.

In this Letter, we investigate the atomistic mechanism and ultrafast dynamics of nonthermal melting of the most popular semiconductor Si, using nonadiabatic molecular dynamics (MD) simulations based on real-time time-dependent density functional theory (TDDFT). By solving time-dependent Kohn-Sham equations, TDDFT-MD naturally includes nonadiabatic electron-electron scattering and el-ph effects [23]. Realistic optical transitions that reproduce experimental absorption spectrum

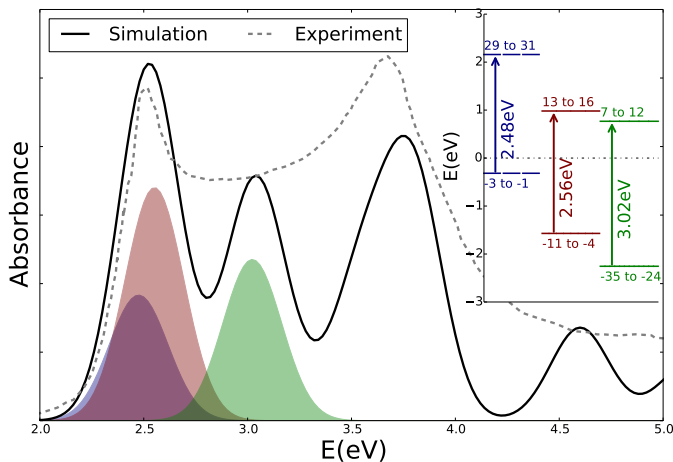


FIG. 1. (Color online) Optical absorption spectrum (transition probability) of Si (solid line). The shadowed zones denote transition probabilities of selected excitation modes. The dash-dot line is experimental spectra red-shifted by a scissor correction of 0.7 eV, adopted from Ref. [28]. (Inset) Corresponding electronic bands of selected excitation modes. The band indexes are relative to the highest occupied state (set as -1).

are invoked. Our parameter-free simulations yield for the first time intrinsic nonthermal melting dynamics of Si, with a ultrafast timescale (200 fs) and a cold lattice ($T < 600$ K). Simulated time evolution of diffraction intensity is almost identically to experimental measurements. Nonthermal melting is attributed to the decrease in bonding electron density and in turn the melting barrier induced by laser illumination, thus in support of the PA mechanism. This work not only builds a general framework to understand nonthermal melting, but also lays down the foundation for reliable simulations of a wide-range of ultrafast physics now by first-principles.

The calculations are performed with a real time TDDFT code, time dependent ab initio package (TDAP) [24] as implemented in SIESTA [25]. Crystalline Si is simulated with a supercell of 64 Si atoms with periodical boundary conditions. The Troullier-Martin pseudopotentials [26] and the adiabatic local density approximation [27] for the exchange-correlation functional are used. An auxiliary real-space grid equivalent to a plane-wave cutoff of 200 Ry is adopted. The Γ point is used to sample the Brillouin zone. During dynamic simulations the evolution time step is 50 as for both electrons and ions in a microcanonical ensemble.

In laser-induced phase transitions the presence of laser pulse greatly modifies atomistic dynamics. According to Runge-Gross theorem [29], the initial state is determinant for many-body dynamics of electronic systems. We thus elaborately build the initial state of photoexcitation by changing the population of Kohn-Sham orbitals from ground state to specific configurations. To be real-

istic, the population variation is proportional to optical transition probability. Laser induced changes in electron density $\Delta\rho(t_0)$ can be expressed as,

$$\Delta\rho(t_0) \propto \sum_{\langle i,j \rangle} P_{ij} (|\psi_i(t_0)|^2 - |\psi_j(t_0)|^2). \quad (1)$$

The transition probability P_{ij} from the initial state $|\psi_i\rangle$ to final state $|\psi_j\rangle$ fulfil Fermi's golden rule:

$$P_{ij} = \left| \langle \psi_i | \epsilon \cdot \hat{P} | \psi_j \rangle \right|^2 \delta(\varepsilon_i - \varepsilon_j - \hbar\omega_l), \quad (2)$$

where $\langle \psi_i | \epsilon \cdot \hat{P} | \psi_j \rangle$ is the transition matrix element, ϵ is the amplitude of electric field, \hat{P} is the momentum operator, ω_l is laser frequency, ε_i and ε_j are the energies of the state $|\psi_i\rangle$ and $|\psi_j\rangle$, respectively. Since DFT usually underestimates the band gap, a scissor correction of 0.7 eV is applied when comparing to experimental absorption spectrum, see Fig. 1. The eigenstates involved in these optical transitions are also shown in the inset. Good agreement between theoretic and experimental absorption spectrum is clearly seen. This method is similar to that proposed by Murray and Fahy in the study of photoexcitation in Bi [30]. We thus built a physical initial state for photoexcited Si, reflecting realistic consequences after laser absorption.

We simulate nonthermal melting of Si under experimental conditions [3]. In experiments laser with a wavelength $\lambda_l = 387$ nm is used [3], corresponding to a photon energy of 2.6 eV here after scissor correction. Without laser illumination, the system reaches a temperature of ~ 300 K quickly. With laser excitation about 10.16% valence electrons can be pumped to the conduction bands. Here we use the percentage of valence electrons pumped to denote the laser intensity η .

We analyze radial distribution function (RDF) of Si-Si bonds at $t = 25, 50, 100, 300$ fs after excitation with $\eta = 10.16\%$ and $\eta = 0\%$. As shown in Fig. 2(a-d), the RDF for the $\eta = 10.16\%$ case shows the features of melting: the first peak shifts right, implying the increase in the nearest neighbor distance; and all peaks become diffusive, indicating a broken crystalline order. For a quantitative evaluation, we adopt the Lindemann criterion: Si melts when its root mean square displacement (RMSD) $\langle u^2(t) \rangle^{\frac{1}{2}}$ is larger than the critical value $R_c = 0.35 \text{ \AA}$ [21]. The RMSD with and without laser are shown in Fig. 2(f). The maximum RMSD without laser ($\eta = 0\%$) reaches only half of R_c . However, the RMSD with laser intensity $\eta = 10.16\%$ crosses the R_c in 100 fs and keep increasing to about 0.6 \AA within 400 fs, showing an evident ultrafast melting behavior.

The RMSD is directly connected to diffraction intensity $I(t)$ through the Debye-Waller formula:

$$I(t) = \exp[-Q^2 \langle u^2(t) \rangle / 3], \quad (3)$$

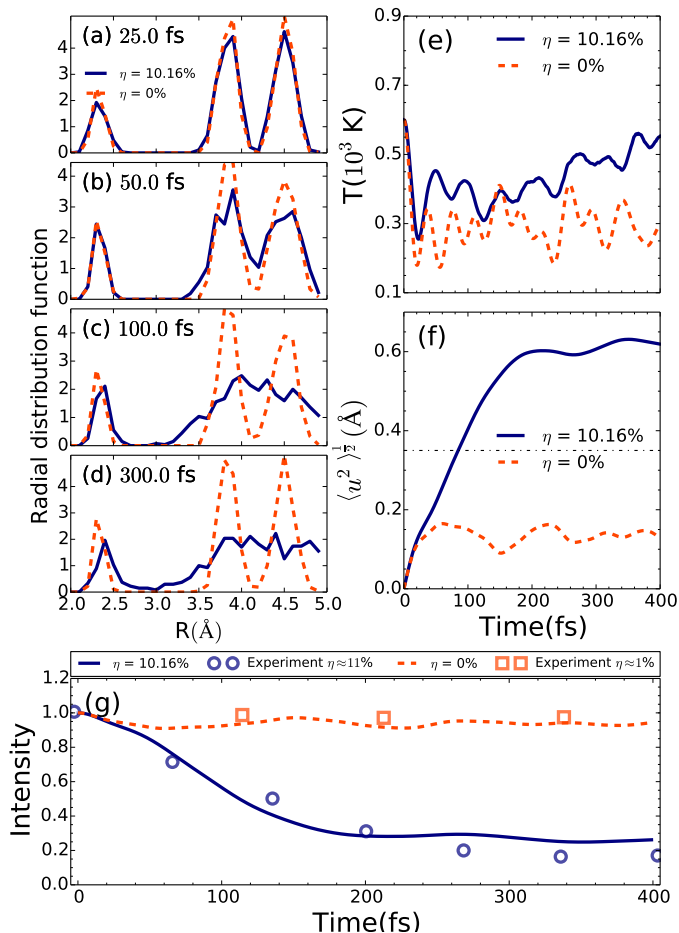


FIG. 2. (Color online) (a-d) Evolution of RDF. (e) Ionic temperature as a function of time. (f) RMSD as a function of time. (g) Simulated and experimental electron diffraction intensity of (220) reflection as a function of time. Experimental data (time rescaled by a factor of 0.33) are taken from Ref. [3].

where Q is the reciprocal lattice vector of the probed reflection, $\langle u^2(t) \rangle$ is the mean square displacement, i.e. the square of RMSD. We simulate the $I_{\eta=10.16\%}(t)$ and $I_{\eta=0\%}(t)$ for the (220) reflection as shown in Fig. 2(g). The features of experimental data [3] and our simulations are almost identical. The $I_{\eta \sim 11\%}(t)$ decreases to 0.22 after melting in both experiment and our simulation. While without laser, both the simulated and experimental $I_{\eta \sim 0\%}(t)$ shows no drift but an oscillation around 0.95. It demonstrates that our simulation captures the most important features of nonthermal melting observed in experiment. The only difference is that in our simulation the melting speed is even faster, possibly because of the small supercell size used in the simulation and other complications in experiment including surface effects and a large pulse width used (200 fs).

The nonadiabatic el-ph effects play a crucial role in nonthermal energy transfer. In our simulations the increase in ionic kinetic energy is compensated by the

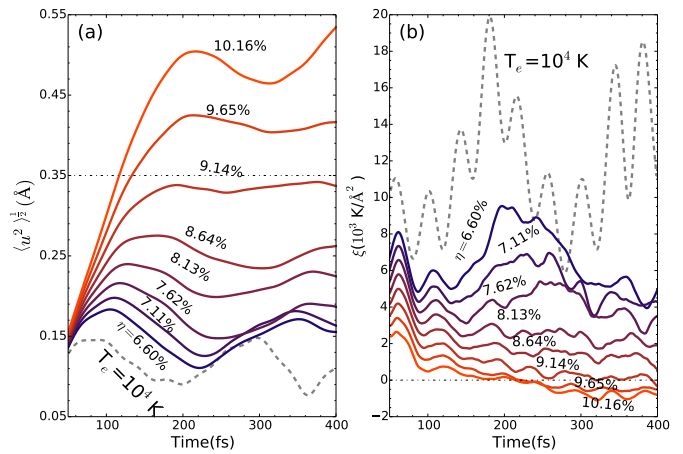


FIG. 3. (Color online) The (a) RMSD and (b) ξ as a function of time under different laser intensities.

decrease in electronic Kohn-Sham energy, so that the total energy of the system is conserved [31]. Overall, only slight increase in ionic temperature is observed. As shown in Fig. 2(e), the system is slightly heated to 550 K after 400 fs upon excitation. The lattice remains cold compared to thermal melting temperature of 1680 K. This suggests el-ph coupling introduces only a small el-ph energy transfer before Si melts. It is consistent with the widely accepted picture that el-ph scattering is insufficient to increase ionic temperature substantially within the subpicosecond time scale [4, 17]. Therefore nonthermal melting of Si in a “cold” lattice is demonstrated, which is radically different from regular thermal melting at 1680 K.

To understand why nonthermal melting could occur, we adopt a simplest model to evaluate the energy barrier for melting. We use a harmonic potential to represent the interatomic interaction, similar to that in Ref. [7]. Since the total energy is conserved during melting, the increase in potential energy $\Delta E_p(t) \propto \langle u^2(t) \rangle$ equals the decrease in ionic kinetic energy $\Delta E_k(t) \propto \Delta T(t) = T(t_0) - T(t)$. Thus we obtain $\xi \langle u^2(t) \rangle \equiv \Delta T(t)$, where ξ is a constant.

If melting occurs with $\langle u^2(t) \rangle^{1/2} = R_c$, the temperature needed for melting is approximately $T_c \geq \Delta T = \xi R_c^2$, and the barrier is estimated as $k_B T_c = \xi k_B R_c^2$, where k_B is the Boltzmann constant.

Figure 3 displays the evolution of RMSD and ξ under different laser intensities. We find that the maximum of RMSD increases as the laser intensity increases. A critical intensity $\eta_c = 9.14\%$ is found when the RMSD just reaches $R_c = 0.35$ Å. It agrees well with the threshold intensity of 5-10% for laser induced melting found in experiment [17].

Consequently, as laser intensity increases, the nominal melting barrier ξ decreases (Fig. 3(b)). For laser intensity $\eta = 10.16\%$, maximum ξ at $t \sim 60$ fs is 2.4×10^3 K/Å²,

TABLE I. The total excitation energy and the charge transfer Δn . The experimental excitation energy is evaluated as $E = \eta_{\text{exp}} E_g$, where $\eta_{\text{exp}} = 11\%$ is the experimental percentage of the excited electrons from Ref. [3] and $E_g = 2.6$ eV is the direct band gap of Si after scissor correction.

System	Energy(eV/electron)	Δn (e/atom)
This work ($\eta = 10.16\%$)	0.28	0.104
TTM ($T_e = 10^4$ K)	0.33	0.045
TTM ($T_e = 2.5 \times 10^4$ K)	1.25	0.112
Experiment [3]	0.29	-

meaning only a temperature $T = 294$ K is needed to reach melting with $R_c = 0.35$ Å. Thus Si melts at room temperature, much lower than thermal melting point of 1680 K. During melting the loss in ion kinetic energy is compensated by energy transfer from electrons to ions via el-pl scattering. Thus ξ become negative after $t = 220$ fs. This interesting phenomenon can only be observed in TDDFT simulations with nonadiabatic effect included.

The shrinking melting barrier upon excitation is further attributed to laser induced bond weakening. To illustrate its electronic origin, we display in Fig. 4 laser induced charge density difference $\Delta\rho$. Comparing $\Delta\rho$ for $\eta = 10.16\%$ (Fig. 4(f)) with $\Delta\rho$ in the bonding state (Fig. 4(c)), we find that laser pulses induce electron transfer from the bonding state to antibonding state, thus significantly lowering the melting barrier. The amount of charge transfer can be evaluated by $\Delta n = (1/2N_a) \int_v |\Delta\rho| d^3r$, where v is the volume and N_a is the number of atoms in the unit cell. As shown in Table I, $\Delta n = 0.104$ e/atom is transferred from the bonding state to antibonding state with laser intensity $\eta = 10.16\%$, accounting for the barrier decrease in laser excited Si.

Phonon dispersion analysis further confirms that upon laser excitation both the longitudinal acoustic (LA) and transverse acoustic (TA) phonon modes destabilize (Fig. 5). For laser intensity $\eta > 1\%$, negative frequencies show up all over the Brillouin zone, especially along $\Gamma - X$ and $\Gamma - \Delta$ directions. Severe phonon softening leads to ultrafast melting. Note that phonon instability calculated from physical excitation conditions is much stronger than that predicted in TTM models, where only TA modes are softened [21]. The latter is inconsistent with experimental analysis that all phonons are affected [7].

The widely used TTM based on BOA yields radically different behaviors. The maximum laser energy in experiment is estimated to be 0.29 eV per valence electron, similar to the energy gain with an electronic temperature $T_e = 10^4$ K (Table I). However, no melting is observed with $T_e = 10^4$ K, whose temperature and RMSD is shown in Fig. 4. The RMSD is only 0.1 Å, far below $R_c = 0.35$ Å. This is resulted from insufficient excitation in TTM: the Δn for $T_e = 10^4$ K is only half that for

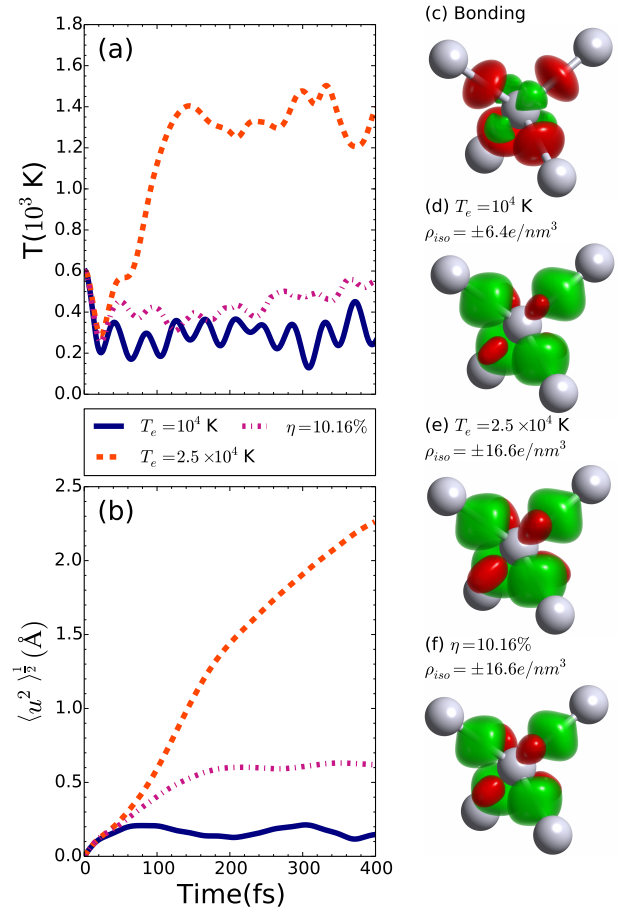


FIG. 4. (Color online)(a) Ionic temperature as a function of time. (b) The RMSD as a function of time. (c) Charge density difference between the ground state and the superposition of atomic charge densities. (d-f) Charge density difference induced by laser excitation in TTM and TDDFT. The red (green) region represents density increase (decrease) in charge density.

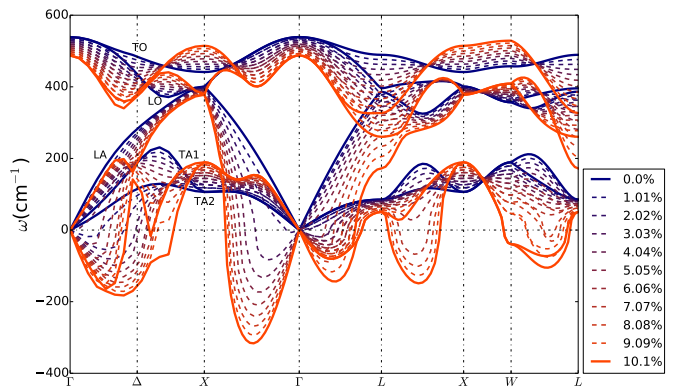


FIG. 5. (Color online) Phonon dispersion spectra of Si under different laser intensities.

$\eta = 10.16\%$, see Fig. 4(d,f) and Table I. Consequently, Si bonds are not sufficiently weakened and melting barrier is overestimated. From Fig. 3(b), the average $\xi_{T_e=10^4 K}$ is $1.3 \times 10^4 \text{ K}/\text{\AA}^2$, much larger than $\xi_{\eta=10.16\%}$. To reach $R_c = 0.35 \text{ \AA}$, a temperature $T = 1593 \text{ K}$ is needed, close to thermal melting temperature 1680 K . Thus, there is no nonthermal melting in the TTM simulations.

A previous study reported that Si melts with a much higher $T_e = 2.5 \times 10^4 \text{ K}$ [18]. In this case, the Δn value is close to that for $\eta = 10.16\%$. However, the RMSD rapidly increases unreasonably to 2.3 \AA in 400 fs, much larger than 0.6 \AA as observed in experiment [3]. More importantly, lattice temperature rapidly increases to $T > 1400 \text{ K}$ in 160 fs, which is a common feature of TTM reported also for Ge melting [19], implying a thermal process. After all, the energy required to reach $T_e = 2.5 \times 10^4 \text{ K}$ is ~ 4 times larger than the energy input from laser pulses (Table I), violating energy conservation law [31, 32].

In conclusion, we have investigated nonthermal melting of Si using TDDFT, where physical excitation conditions and nonadiabatic effects are naturally included. Without adjustable parameters the simulation shows ultrafast melting behavior, in excellent agreement with experimental measurements in terms of laser threshold and decay of diffraction intensity. During laser melting the crystal lattice remains cold ($T < 600 \text{ K}$), suggesting a nonthermal phenomenon, which is further attributed to drastic laser-induced changes in bonding electron density and subsequent decrease in melting barrier. Thus, we validate the PA mechanism of nonthermal melting speculated 30 years ago, and provide further dynamic prospects. The novel approach could be extended to study other nonthermal phenomena of materials.

We acknowledge financial supports from MOST (grants 2012CB921403 and 2015CB921001) and NSFC (grant 11222431). SBZ was supported by the Department of Energy under Grant No. DE-SC0002623.

* zhangs9@rpi.edu

† smeng@iphy.ac.cn

- [1] K. K. Ostrikov, F. Beg, and A. Ng, *Rev. Mod. Phys.* **88**, 011001 (2016).
- [2] C. V. Shank, R. Yen, and C. Hirlimann, *Phys. Rev. Lett.* **50**, 454 (1983).
- [3] M. Harb, R. Ernstorfer, T. Dartigalongue, C. T. Hebeisen, R. E. Jordan, and R. D. Miller, *J. Phys. Chem. B* **110**, 25308 (2006); M. Harb, R. Ernstorfer, C. T. Hebeisen, G. Sciaini, W. Peng, T. Dartigalongue, M. A. Eriksson, M. G. Lagally, S. G. Kruglik, and R. J. D. Miller, *Phys. Rev. Lett.* **100**, 155504 (2008).
- [4] C. W. Siders, A. Cavalleri, K. Sokolowski-Tinten, C. Tóth, T. Guo, M. Kammler, M. H. v. Hoegen, K. R. Wilson, D. v. d. Linde, and C. P. J. Barty, *Science* **286**, 1340 (1999); A. Cavalleri, C. W. Siders, F. L. H. Brown, D. M. Leitner, C. Tóth, J. A. Squier, C. P. J. Barty, K. R. Wilson, K. Sokolowski-Tinten, M. Horn von Hoegen, D. von der Linde, and M. Kammler, *Phys. Rev. Lett.* **85**, 586 (2000); K. Sokolowski-Tinten, C. Blome, C. Dietrich, A. Tarasevitch, M. Horn von Hoegen, D. von der Linde, A. Cavalleri, J. Squier, and M. Kammler, *Phys. Rev. Lett.* **87**, 225701 (2001).
- [5] E. N. Glezer, Y. Siegal, L. Huang, and E. Mazur, *Phys. Rev. B* **51**, 9589 (1995).
- [6] K. Sokolowski-Tinten, J. Bialkowski, and D. von der Linde, *Phys. Rev. B* **51**, 14186 (1995).
- [7] A. M. Lindenberg, I. Kang, S. L. Johnson, T. Missalla, P. A. Heimann, Z. Chang, J. Larsson, P. H. Bucksbaum, H. C. Kapteyn, H. A. Padmore, R. W. Lee, J. S. Wark, and R. W. Falcone, *Phys. Rev. Lett.* **84**, 111 (2000); A. M. Lindenberg, J. Larsson, K. Sokolowski-Tinten, *et al.*, *Science* **308**, 392 (2005); P. B. Hillyard, K. J. Gaffney, A. M. Lindenberg, *et al.*, *Phys. Rev. Lett.* **98**, 125501 (2007).
- [8] A. Rousse, C. Rischel, S. Fourmaux, I. Uschmann, S. Sebban, G. Grillon, P. Balcou, E. Förster, J.-P. Geindre, P. Audebert, *et al.*, *Nature* **410**, 65 (2001).
- [9] X.-B. Li, X. Q. Liu, X. Liu, D. Han, Z. Zhang, X. D. Han, H.-B. Sun, and S. B. Zhang, *Phys. Rev. Lett.* **107**, 015501 (2011).
- [10] L. Waldecker, T. A. Miller, M. Rudé, R. Bertoni, J. Osmond, V. Pruneri, R. E. Simpson, R. Ernstorfer, and S. Wall, *Nat. Mater.* **14**, 991 (2015).
- [11] E. Möhr-Vorobeva, S. L. Johnson, P. Beaud, U. Staub, R. De Souza, C. Milne, G. Ingold, J. Demsar, H. Schaefer, and A. Titov, *Phys. Rev. Lett.* **107**, 036403 (2011).
- [12] S. Hellmann, M. Beye, C. Sohrt, T. Rohwer, F. Sorgenfrei, H. Redlin, M. Kalläne, M. Marczyński-Bühlow, F. Hennies, M. Bauer, A. Föhlich, L. Kipp, W. Wurth, and K. Rossnagel, *Phys. Rev. Lett.* **105**, 187401 (2010).
- [13] R. Ernstorfer, M. Harb, C. T. Hebeisen, G. Sciaini, T. Dartigalongue, and R. J. D. Miller, *Science* **323**, 1033 (2009).
- [14] P. M. Leguay, A. Lévy, B. Chimier, F. Deneuville, D. Descamps, C. Fourment, C. Goyon, S. Hulin, S. Petit, O. Peyrusse, J. J. Santos, P. Combis, B. Holst, V. Recoules, P. Renaudin, L. Videau, and F. Dorchies, *Phys. Rev. Lett.* **111**, 245004 (2013).
- [15] S. Juodkakis, K. Nishimura, S. Tanaka, H. Misawa, E. G. Gamaly, B. Luther-Davies, L. Hallo, P. Nicolai, and V. T. Tikhonchuk, *Phys. Rev. Lett.* **96**, 166101 (2006).
- [16] L. Rapp, B. Haberl, C. Pickard, J. Bradby, E. Gamaly, J. Williams, and A. Rode, *Nat. Commun.* **6**, 7555 (2015).
- [17] S. Sundaram and E. Mazur, *Nat. Mater.* **1**, 217 (2002).
- [18] P. L. Silvestrelli, A. Alavi, M. Parrinello, and D. Frenkel, *Phys. Rev. Lett.* **77**, 3149 (1996).
- [19] P. Ji and Y. Zhang, *J. Phys. D: Appl. Phys.* **46**, 495108 (2013).
- [20] N. Medvedev, H. O. Jeschke, and B. Ziaja, *New J. Phys.* **15**, 015016 (2013); N. Medvedev, Z. Li, and B. Ziaja, *Phys. Rev. B* **91**, 054113 (2015).
- [21] E. S. Zijlstra, J. Walkenhorst, and M. E. Garcia, *Phys. Rev. Lett.* **101**, 135701 (2008); E. S. Zijlstra, A. Kalitsov, T. Zier, and M. E. Garcia, *Phys. Rev. X* **3**, 011005 (2013).
- [22] P. B. Hillyard, D. A. Reis, and K. J. Gaffney, *Phys. Rev. B* **77**, 195213 (2008).
- [23] M. A. Marques, N. T. Maitra, F. M. Nogueira, E. Gross, and A. Rubio, *Fundamentals of Time-Dependent Density*

- Functional Theory* (Springer Berlin Heidelberg, 2012).
- [24] S. Meng and E. Kaxiras, *J. Chem. Phys.* **129**, 054110 (2008).
- [25] P. Ordejón, E. Artacho, and J. M. Soler, *Phys. Rev. B* **53**, R10441 (1996); J. M. Soler, E. Artacho, J. D. Gale, A. García, J. Junquera, P. Ordejón, and D. Sánchez-Portal, *J. Phys. Condens. Matter* **14**, 2745 (2002); D. Sánchez-Portal, P. Ordejón, E. Artacho, and J. M. Soler, *Inter. J. Quantum. Chem.* **65**, 453 (1997).
- [26] N. Troullier and J. L. Martins, *Phys. Rev. B* **43**, 8861 (1991).
- [27] J. P. Perdew and A. Zunger, *Phys. Rev. B* **23**, 5048 (1981).
- [28] P. Lautenschlager, M. Garriga, L. Vina, and M. Cardona, *Phys. Rev. B* **36**, 4821 (1987).
- [29] E. Runge and E. K. U. Gross, *Phys. Rev. Lett.* **52**, 997 (1984).
- [30] E. D. Murray and S. Fahy, *Phys. Rev. Lett.* **114**, 055502 (2015).
- [31] See Supplemental Material at URL for details.
- [32] R. M. Wentzcovitch, J. L. Martins, and P. B. Allen, *Phys. Rev. B* **45**, 11372 (1992).